Preprint typeset using LaTeX style emulateapj v. 11/10/09

OPTIMIZING OBSERVING CAMPAIGNS FOR STRONG GRAVITATIONAL LENS TIME DELAYS

Leonidas A. Moustakas & Andrew Romero-Wolf[1]

ABSTRACT

We report on a flexible and extendable inference technique for measuring the time delays between images in time-varying strong gravitational lenses, and for optimizing observational parameters to achieve a target time delay precision. Robust time delays and meaningful estimates of the corresponding uncertainties are essential for using such time delays for several astrophysical applications, including estimating the Hubble constant, other cosmological parameters, or for constraining lens-galaxy structure or substructure properties. Quasar's optical light curves have been shown to be described well by a damped random walk behavior. We build a generative model of paired quasar light curves which are offset by a constant delay and magnitude, and build an inference process using the emcee Markov Chain Monte Carlo engine. With this framework, we explore the problem of designing observational campaigns that will achieve time delay measurements at a specific threshold level. We apply this approach to a notional *Hubble* Space Telescope lens-monitoring experiment, to determine the observing campaign characteristics and photometric sensitivity that are required to secure a greater than 90% probability of measuring a 1.5-day time delay to a combined random and systematic precision of better than one hour, a more than twenty-fold improvement of what is presently achieved. We discuss the extensibility of this approach to other experimental designs, including from short-cadence, focused ground-based campaigns.

Subject headings: gravitational lensing — cosmology: dark matter

1. INTRODUCTION

Gravitational lensing time delays are a promising tool for measuring Hubble's constant (H_0; Refsdal 1964) as well as dark energy cosmological parameters (Coe & Moustakas 2009; Linder 2011; Treu et al. 2013), with compelling complementarity to other techniques (Weinberg et al. 2013; Linder 2015). Indeed, there is presently tension in the value for H_0 inferred by the *Planck* cosmic microwave background analysis (Planck Collaboration et al. 2014, 2015), and the best-determined values derived through sophisticated modeling of gravitational lenses that include time delay information (e.g. Suyu et al. 2013, 2014).

Such measurements depend on detailed modeling of often complex gravitational environments and material along the line of sight (e.g. Greene et al. 2013; Schneider & Sluse 2013), but the foundation is the time delay measurement itself, which depends on the details of the observational campaign timing and duration, and the associated photometric measurements of each individual image in a lens. Substantial campaigns have been undertaken over the past ten or more years (e.g. Eigenbrod et al. 2005; Tewes et al. 2013), achieving time delay precisions of approaching $\sim 1\,\mathrm{day}$[2]. To date, achieving time delays with greater precision has been elusive (e.g. Oguri 2007), due in part by the difficulty of coordinating observing campaigns with better than approximately nightly cadence.

However, with cosmological measurement implications of much more precise and better-characterized time delays, and their potential of being used to infer properties of the dark matter substructure expected to be contained within lensing galaxies (e.g. Primack 2009; Xu et al. 2009), we are driven to understand how to design and analyze observing campaigns that may achieve an order of magnitude higher time delay precision than is currently typical (Keeton & Moustakas 2009; Linder 2011).

This motivates us to develop a time delay measurement technique that can be used both for analysis of existing data, but also for the systematic study of tailored sets of observations and observational characteristics, for optimal design of campaigns, tailored to the needs of the desired scientific goals. Many techniques for fitting time-delayed light curve observations have been explored to date; see the discussion in Dobler et al. (2015) and Liao et al. (2015), for a detailed review.

Since the measurement of the time delay in the first strong gravitational lens discovered, Q0957+561 (Walsh et al. 1979; Press et al. 1992), there have been many significant efforts to systematically monitor time domain variations in multiply imaged quasars, particularly in radio (e.g. Fassnacht et al. 1999) and optical wavelengths (c.f. compilations in Oguri 2007; Mosquera & Kochanek 2011). The near future shows great potential for both vast numbers of poorly-measured time delays (with the Large Synoptic Survey Telescope), and for exquisitely-measured time delays (e.g. using focused Las Cumbres Observatory Global Telescope campaigns, the *Hubble* Space Telescope, or another space-based platform such as the proposed Observatory for Multi-Epoch Gravitational Lens Astrophysics, Moustakas et al. 2008). In either scenario, we wish to be in a position where one may determine precisely how to achieve a *desired* time delay precision with a specific level of certainty.

In this work, we take advantage of a predictive model for the time variations of quasar light curves, to set up a Bayesian inference framework. This is developed in Sec-

[1] Jet Propulsion Laboratory, California Institute of Technology, 4800 Oak Grove Dr, M/S 169-506, Pasadena, CA 91109

[2] COSMOGRAIL webpage, http://http://cosmograil.org

tion 2, based on descriptions of simulated quasar light curve pairs for particular observational campaign and measurement precision conditions. A notional experimental design is developed in Section 3, to demonstrate our framework's application to achieving a desired time delay precision at a specific confidence level. We discuss the results, and extensions of this methodology to other experiments in Section 4. All code is written in python, and is version-controlled via a github repository.

2. INFERENCE ANALYSIS FRAMEWORK

We concentrate on optical, radio-quiet quasars, whose variability behavior has been shown to be consistent with a damped random walk process, where the fluctuations have a characteristic amplitude and decay time that correlate with the black hole mass and luminosity (MacLeod et al. 2010; Kelly et al. 2009). We refer to these as light curve structure parameters in the discussion that follows. The damped random walk parameters that describe a quasar light curve include an average magnitude $\langle m \rangle$; a short-time variability parameter σ, in units of mag day$^{-1/2}$; and a long-term relaxation time-scale τ, in days. Given a magnitude x_i at time t_i, the magnitude x_{i+1} at time t_{i+1} is given by

$$\begin{aligned} x_{i+1} &= \langle m \rangle \\ &+ e^{-(t_{i+1}-t_i)/\tau} \left(x_i - \langle m \rangle\right) \\ &+ \sigma e^{-(t_{i+1}-t_i)/\tau} \int_0^{t_{i+1}-t_i} e^{s/\tau} dB(s), \end{aligned} \tag{1}$$

where $dB(s)$ is a temporally uncorrelated normally distributed random variable with zero mean and variance dt. The integral over the Gaussian distributed random numbers $dB(s)$ is the "random walk" part of the model while the exponential with constant τ provides the "dampening." The first magnitude value x_1 in a randomly generated series is obtained by taking the limit of $t_1 - t_0 \to \infty$, which results in a gaussian distributed variable with mean $\langle m \rangle$ and variance $\tau\sigma^2/2$. The dependence of the quasar light curve parameters σ and τ on its black hole mass is discussed in Kelly et al. (2009). The damped random walk behavior is likely driven by stochastic thermal processes in their accretion disks. Assuming that this is a reasonable assumption for the timescales of variations under consideration, we use this as the model prescription so we can directly connect the model parameters $\mathbf{m}$ to the data observables $\mathbf{d}$, via Bayes' equation:

$$p(\mathbf{m}|\mathbf{d}) = \frac{p(\mathbf{d}|\mathbf{m})\, p(\mathbf{m})}{p(\mathbf{d})}.$$

In our application, $\mathbf{d}$ is a collection of observed magnitudes x_i with photometric uncertainties σ_i at times t_i. We denote the set of data values by $X = \{(t_i, x_i, \sigma_i)\}$. The model parameters $\mathbf{m}$ are the quasar light curve variation parameters ($\langle m \rangle$, σ, τ). The probability distribution $p(\mathbf{d}|\mathbf{m})$ corresponding to the light curve model given by Equation 1, is

$$p(X|\langle m \rangle, \sigma, \tau) = \prod_{i=1}^{n} \frac{\exp\left(-\frac{1}{2}\frac{(\hat{x}_i - x_i^*)^2}{\Omega_i + \sigma_i^2}\right)}{\sqrt{2\pi\left(\Omega_i + \sigma_i^2\right)}}, \tag{2}$$

where

$$\begin{aligned} x_i^* &= x_i - \langle m \rangle \\ \hat{x}_0 &= 0 \\ \Omega_0 &= \frac{\tau\sigma^2}{2} \\ \hat{x}_i &= a_i \hat{x}_{i-1} + \frac{a_i \Omega_{i-1}}{\Omega_{i-1} + \sigma_{i-1}^2}\left(x_{i-1}^* - \hat{x}_{i-1}\right) \\ \Omega_i &= \Omega_0\left(1 - a_i^2\right) + a_i^2 \Omega_{i-1}\left(1 - \frac{\Omega_{i-1}}{\Omega_{i-1} + \sigma_{i-1}^2}\right), \end{aligned} \tag{3}$$

and

$$a_i = e^{-(t_i - t_{i-1})/\tau}.$$

The prior distribution of model values $p(\mathbf{m})$ is determined by the extent of existing measurements or theoretical expectations, while the probability distribution of the data $p(\mathbf{d})$ is treated as a normalization factor.

We implement this in two ways; first to analyze a single time-stream of observations, towards estimating the structure parameters of the light curve; and second, to analyze combined pairs of ostensibly correlated light curves, to determine the combination of the structure parameters and the offset parameters that best join the light curves. The likelihood function used to reconstruct the quasar light curve damped random walk parameters is

$$\log \mathcal{L}_K(X|\langle m \rangle, \sigma, \tau) = - \frac{1}{2}\sum_{i=1}^{n}\left\{\frac{(\hat{x}_i - x_i^*)^2}{\Omega_i + \sigma_i^2} + \log\left[2\pi\left(\Omega_i + \sigma_i^2\right)\right]\right\}. \tag{4}$$

The offset light curves of two images of a single intrinsic quasar's light curve are merged according to a hypothesized delay and magnitude (or multiplicative-flux) offset. In other words, given a set of light curves $X_1 = \{(t_i, x_{1,i}, \sigma_{1,i})\}$ and $X_2 = \{(t_i, x_{2,i}, \sigma_{2,i})\}$, observed with the same time sample t_i, we map the points in X_2 to $X_2' = \{(t_i - \Delta t, x_{2,i} - \Delta m, \sigma_{2,i})\}$ such that the merged data X_1 and X_2', denoted by $M(\Delta t, \Delta m; X_1, X_2)$ is best described by a single light curve model. The likelihood for the merged lightcurves under a hypothesis ($\Delta t, \Delta m$) and ($\langle m \rangle$, τ, and σ) is given by

$$\begin{aligned} &\mathcal{L}(X_1, X_2|\Delta t, \Delta m, \sigma, \tau, \langle m \rangle) = \\ &\mathcal{L}_K\left(M(\Delta t, \Delta m; X_1, X_2)|\sigma, \tau, \langle m \rangle\right), \end{aligned} \tag{5}$$

with a posterior probability given by

$$\begin{aligned} p(\Delta t, \Delta m, \langle m \rangle, \sigma, \tau|X_1, X_2) \propto \\ \mathcal{L}(X_1, X_2|\Delta t, \Delta m, \langle m \rangle, \sigma, \tau) \times \\ p(\Delta t, \Delta m, \langle m \rangle, \sigma, \tau). \end{aligned} \tag{6}$$

The assignement of priors is flat in Δt. The parameters σ and τ are scale parameters, so their priors are given by $p(\sigma) = \sigma^{-1}$ and $p(\tau) = \tau^{-1}$. The parameters $\langle m \rangle$ and Δm are also scale parameters but as they are logarithmic, we assign them flat priors.

With the posterior probability expression, we can now use a Markov Chain Monte Carlo (MCMC) algorithm to explore the likelihood space of the model parameters,

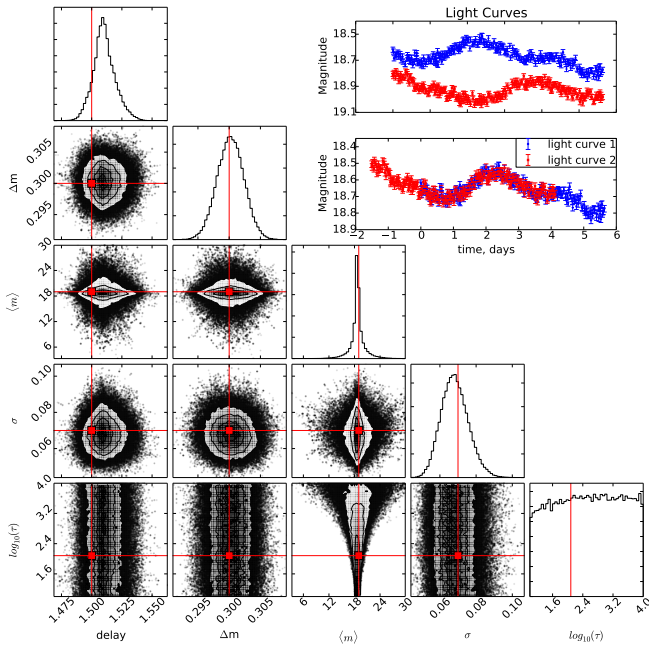

FIG. 1.— Markov Chain Monte Carlo (MCMC) results for an example for the parameter reconstruction of a light curve and its delayed and magnitude offset image. The quasar light curve parameters τ, σ and $\langle m \rangle$ are estimated under a hypothesis value for the delay and Δm. On the top right the quasar light curve (blue) and its delayed magnitude offset image (red) are shown with the image delay and magnitude offset corrected from the most probable values of the delay and Δm distributions. The quasar light curve parameters are $\langle m \rangle$=19.0 magnitudes, σ=0.07 mag day$^{-1/2}$ and τ=121 days. In this example, the observations were modeled with a photometric uncertainty of 0.02 magnitudes. Truth values are shown as red lines overlaid on the sampled distributions.

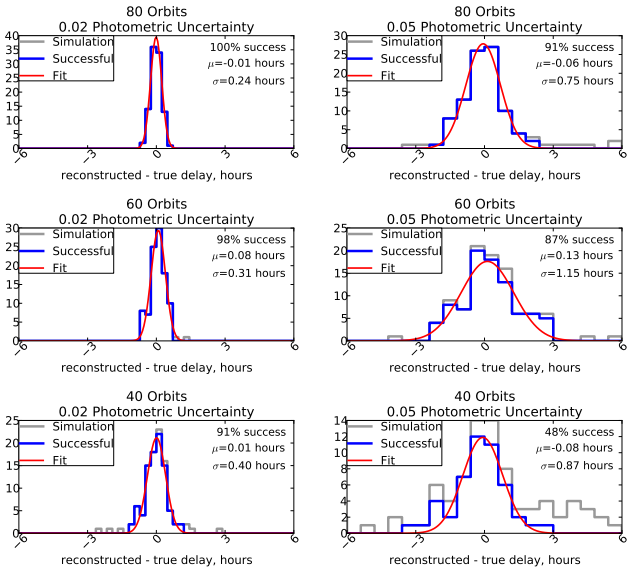

FIG. 2.— The probability of a successful measurement and resolution are shown for several examples of number of orbits and photomoetric uncertainty. The delay residuals from the simulations are shown in gray. The distribution of successful instances, with the requirements described in the text, are shown in blue. A Gaussian function is fit to the distribution of successful delay reconstructions for a convenient estimate of the final (non-outlier) time delay measurement fidelity.

based on specified observational parameters. We use the Affine Invariant MCMC sampler algorithm of Foreman-Mackey et al. (2013), and the triangle plotting algorithm Dan Foreman-Mackey and Adrian Price-Whelan and Geoffrey Ryan and Emily and Michael Smith and Kyle Barbary and David W. Hogg and Brendon J. Brewer (2014). In Figure 1 we show a sample generated pair of light curves drawn for the same intrinsic quasar light curve properties, with a time delay of Δt=1.5 day and a magnitude offset of Δm=0.3 magnitudes. To make the scenario more specific, we consider a system similar to RX J1131-1231 (Sluse et al. 2003), whose estimated black hole mass of $\sim 10^8\,M_\odot$ (Dai et al. 2010), and estimate $\sigma \approx 0.56$ and $tau \approx 121$ using the correlations in MacLeod et al. (2010). The triangle-plot shows the posterior likelihood distributions the delay parameters (Δt, Δm) and the light curve structure parameters ($\langle m \rangle$, σ, τ), including their marginalized distributions.

3. AN EXPERIMENTAL DESIGN

To test our approach we explore what observational design parameters would be required to achieve a greater than 90% probability of measuring a 1.5 day time delay, to a combined random and systematic precision of better than 1.0 hour. To make this exploration more concrete, we assume space-quality high resolution observations (e.g. with the *Hubble* Space Telescope; *HST*), to confidently be able to assume completely independent non-overlapping photometric measurements of each image in our notional gravitational lens, and photometric stability that may be more robustly assumed to be stable to at least $\sim 1\%$. For the purposes of this setup, we adopt the *HST* "orbit" as a natural unit of time, which equals ~ 90 minutes.

In nature, one set of observations may accurately represent our statistical description of a process, but that set may or may not in itself contain enough information to allow a clear inference of the details of the underlying process. To test the efficacy of a planned experimental design, so we can confidently forecast the probability of success, an understanding of the likely nature of outlier measurements, and the performance as a function of the specific target values for each observational constraint, we generate a large set of simulated observations drawn from the same observational characteristics, and do the full inference analysis on each of these. The results from such a Monte Carlo exploration of an experimental setup are shown in Figure 2, for the set of observational choices shown in the same Figure.

The cuts required by for a valid reconstruction are described as follows. We fit a Gaussian curve to the distribution of 100 simulation delay results (see Figure 2). We have found that the python SciPy curve_fit method, which employs the Levenberg-Marquardt algorithm, is not driven by outliers. The standard deviation σ from the fit is used to reject reconstruction results by requiring that a reconstructed delay be within 3σ of the true delay. We also require that the uncertainty in the delay, obtained from the posterior distribution of the MCMC process (see the top left panel of Figure 1 for an example), to be within 3σ to reject poor reconstructions. We define the success as the fraction of light curve delay reconstructions surviving these cuts.

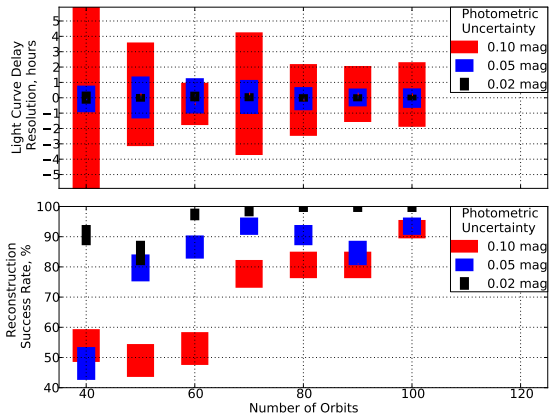

FIG. 3.— Summary of results for the delay measurement resolution (top panel) reconstruction success rate (bottom panel). Photometric uncertainties of 0.02 mag result in delay resolutions smaller than one day and are down to six hours for 80 orbits and above. Even with photometric uncertainties of 0.05 mag, delay resolutions smaller that 1 day can be achieved. The reconstruction success is 90% for more than 60 orbits and photometric uncertainties below 0.05 mag.

4. DISCUSSION AND CONCLUSIONS

We discuss the lessons from our analysis and the process of having designed an experiment, with an emphasis on the possible pitfalls. The way that the priors are set up, and carefully establishing enough burn-in chains in the MCMC process, are important. For a consistency check, we can analyze each image's timestream separately as well as jointly, and compare derived values for the light curve structure parameters. We have also implicitly assumed that the photometric measurement uncertainties are uncorrelated, which may not be the case for e.g. deconvolved ground-based observations. However, it is straightforward to incorporate such covariances in our analysis.

The setup in Section 3, by concentrating on a relatively short intrinsic time delay, largely avoids the effect that stochastic microlensing variations in one or both of the images would have. This is a variational component that can be included with additional parametrizations in our model, and will be the topic of future work. Isolating and characterizing the microlensing signal in long-term monitoring observations of lenses is important in its own right, because it can be used as an additional measurement of the internal smooth dark matter component in lensing galaxies (Schechter & Wambsganss 2002), as well as a probe for the detailed structure of the quasar accretion disk (e.g. Morgan et al. 2010).

A key assumption in this analysis is that the generative function adopted for the light curves is appropriate. The damped random walk may not fully describe the variation behavior on short (sub-day) timescales, as discussed by Zu et al. (2013) and Mushotzky et al. (2011), based on ground- and space-based data, respectively (OGLE and *Kepler*). A systematic examination of this issue is the topic of future work.

The method developed here has been applied to the Time Delay Challenge exercise (references here; marked there as the "JPL" contributor), which emulates data similar to what is expected from the Large Synoptic Survey Telescope (LSST). As those are expected to be extremely long time-streams (extending to years), microlensing was a significant element in many of the light curves, which impacted our performance. A new "grander" time delay challenge is being discussed, with a focus on achieving absolute precision time delay measurements that are more on the order of the experimental setup of Section 3.

This work was carried out at Jet Propulsion Laboratory, California Institute of Technology, under a contract with NASA. We are grateful for conversations with Francis-Yan Cyr-Racine, Chuck Keeton, and Frederic Courbin.

REFERENCES

Coe, D. & Moustakas, L. A. 2009, ApJ, 706, 45
Dai, X., Kochanek, C. S., Chartas, G., Kozłowski, S., Morgan, C. W., Garmire, G., & Agol, E. 2010, ApJ, 709, 278
Dan Foreman-Mackey and Adrian Price-Whelan and Geoffrey Ryan and Emily and Michael Smith and Kyle Barbary and David W. Hogg and Brendon J. Brewer. 2014, triangle.py v0.1.1, http://dx.doi.org/10.5281/zenodo.11020
Dobler, G., Fassnacht, C. D., Treu, T., Marshall, P., Liao, K., Hojjati, A., Linder, E., & Rumbaugh, N. 2015, ApJ, 799, 168
Eigenbrod, A., Courbin, F., Vuissoz, C., Meylan, G., Saha, P., & Dye, S. 2005, A&A, 436, 25
Fassnacht, C. D., Pearson, T. J., Readhead, A. C. S., Browne, I. W. A., Koopmans, L. V. E., Myers, S. T., & Wilkinson, P. N. 1999, ApJ, 527, 498
Foreman-Mackey, D., Hogg, D. W., Lang, D., & Goodman, J. 2013, PASP, 125, 306
Greene, Z. S., Suyu, S. H., Treu, T., Hilbert, S., Auger, M. W., Collett, T. E., Marshall, P. J., Fassnacht, C. D., Blandford, R. D., Bradač, M., & Koopmans, L. V. E. 2013, ApJ, 768, 39
Keeton, C. R. & Moustakas, L. A. 2009, ApJ, 699, 1720
Kelly, B. C., Bechtold, J., & Siemiginowska, A. 2009, ApJ, 698, 895
Liao, K., Treu, T., Marshall, P., Fassnacht, C. D., Rumbaugh, N., Dobler, G., Aghamousa, A., Bonvin, V., Courbin, F., Hojjati, A., Jackson, N., Kashyap, V., Rathna Kumar, S., Linder, E., Mandel, K., Meng, X.-L., Meylan, G., Moustakas, L. A., Prabhu, T. P., Romero-Wolf, A., Shafieloo, A., Siemiginowska, A., Stalin, C. S., Tak, H., Tewes, M., & van Dyk, D. 2015, ApJ, 800, 11
Linder, E. V. 2011, Phys. Rev. D, 84, 123529
—. 2015, ArXiv e-prints
MacLeod, C. L., Ivezić, Ž., Kochanek, C. S., Kozłowski, S., Kelly, B., Bullock, E., Kimball, A., Sesar, B., Westman, D., Brooks, K., Gibson, R., Becker, A. C., & de Vries, W. H. 2010, ApJ, 721, 1014
Morgan, C. W., Kochanek, C. S., Morgan, N. D., & Falco, E. E. 2010, ApJ, 712, 1129
Mosquera, A. M. & Kochanek, C. S. 2011, ApJ, 738, 96
Moustakas, L. A., Bolton, A. J., Booth, J. T., Bullock, J. S., Cheng, E., Coe, D., Fassnacht, C. D., Gorjian, V., Heneghan, C., Keeton, C. R., Kochanek, C. S., Lawrence, C. R., Marshall, P. J., Metcalf, R. B., Natarajan, P., Nikzad, S., Peterson, B. M., & Wambsganss, J. 2008, in Society of Photo-Optical Instrumentation Engineers (SPIE) Conference Series, Vol. 7010, Society of Photo-Optical Instrumentation Engineers (SPIE) Conference Series, 1

Mushotzky, R. F., Edelson, R., Baumgartner, W., & Gandhi, P. 2011, ApJ, 743, L12
Oguri, M. 2007, ApJ, 660, 1
Planck Collaboration, Ade, P. A. R., Aghanim, N., Armitage-Caplan, C., Arnaud, M., Ashdown, M., Atrio-Barandela, F., Aumont, J., Baccigalupi, C., Banday, A. J., & et al. 2014, A&A, 571, A16
Planck Collaboration, Ade, P. A. R., Aghanim, N., Arnaud, M., Ashdown, M., Aumont, J., Baccigalupi, C., Banday, A. J., Barreiro, R. B., Bartlett, J. G., & et al. 2015, ArXiv e-prints
Press, W. H., Rybicki, G. B., & Hewitt, J. N. 1992, ApJ, 385, 404
Primack, J. R. 2009, New Journal of Physics, 11, 105029
Refsdal, S. 1964, MNRAS, 128, 307
Schechter, P. L. & Wambsganss, J. 2002, ApJ, 580, 685
Schneider, P. & Sluse, D. 2013, A&A, 559, A37
Sluse, D., Surdej, J., Claeskens, J.-F., Hutsemékers, D., Jean, C., Courbin, F., Nakos, T., Billeres, M., & Khmil, S. V. 2003, A&A, 406, L43
Suyu, S. H., Auger, M. W., Hilbert, S., Marshall, P. J., Tewes, M., Treu, T., Fassnacht, C. D., Koopmans, L. V. E., Sluse, D., Blandford, R. D., Courbin, F., & Meylan, G. 2013, ApJ, 766, 70
Suyu, S. H., Treu, T., Hilbert, S., Sonnenfeld, A., Auger, M. W., Blandford, R. D., Collett, T., Courbin, F., Fassnacht, C. D., Koopmans, L. V. E., Marshall, P. J., Meylan, G., Spiniello, C., & Tewes, M. 2014, ApJ, 788, L35
Tewes, M., Courbin, F., & Meylan, G. 2013, A&A, 553, A120
Treu, T., Marshall, P. J., Cyr-Racine, F.-Y., Fassnacht, C. D., Keeton, C. R., Linder, E. V., Moustakas, L. A., Bradac, M., Buckley-Geer, E., Collett, T., Courbin, F., Dobler, G., Finley, D. A., Hjorth, J., Kochanek, C. S., Komatsu, E., Koopmans, L. V. E., Meylan, G., Natarajan, P., Oguri, M., Suyu, S. H., Tewes, M., Wong, K. C., Zabludoff, A. I., Zaritsky, D., Anguita, T., Brunner, R. J., Cabanac, R., Falco, E. E., Fritz, A., Seidel, G., Howell, D. A., Giocoli, C., Jackson, N., Lopez, S., Metcalf, R. B., Motta, V., & Verdugo, T. 2013, ArXiv e-prints
Walsh, D., Carswell, R. F., & Weymann, R. J. 1979, Nature, 279, 381
Weinberg, D. H., Mortonson, M. J., Eisenstein, D. J., Hirata, C., Riess, A. G., & Rozo, E. 2013, Phys. Rep., 530, 87
Xu, D. D., Mao, S., Wang, J., Springel, V., Gao, L., White, S. D. M., Frenk, C. S., Jenkins, A., Li, G., & Navarro, J. F. 2009, MNRAS, 398, 1235
Zu, Y., Kochanek, C. S., Kozłowski, S., & Udalski, A. 2013, ApJ, 765, 106